PHYSICAL REVIEW D **88,** 025023 (2013)

Time dependence of particle creation from accelerating mirrors

Michael R. R. Good*
Institute of Advanced Studies, Nanyang Technological University, Singapore 639673, Singapore

Paul R. Anderson†
Department of Physics, Wake Forest University, Winston-Salem, North Carolina 27109, USA

Charles R. Evans‡
Department of Physics and Astronomy, University of North Carolina, Chapel Hill, North Carolina 27599, USA
(Received 28 March 2013; published 16 July 2013)

Particle production due to a quantized, massless, minimally coupled scalar field in two-dimensional flat spacetime with an accelerating mirror is investigated, with a focus on the time dependence of the process. We analyze first the classes of trajectories previously investigated by Carlitz and Willey and by Walker and Davies. We then analyze four new classes of trajectories, all of which can be expressed analytically and for which several ancillary properties can be derived analytically. The time dependence is investigated through the use of wave packets for the modes of the quantized field that are in the *out* vacuum state. It is shown for most of the trajectories studied that good time resolution of the particle production process can be obtained.

DOI: 10.1103/PhysRevD.88.025023 PACS numbers: 03.70.+k, 04.62.+v, 04.60.−m

I. INTRODUCTION

As the simplest theoretical manifestation of the dynamical Casimir effect (DCE), the moving mirror model of DeWitt [1] and Davies and Fulling [2,3] describes the disturbance of a field by an accelerated boundary, which results in both particle production and a flux of energy. As the mirror model matured [4–8], it became apparent that accelerating boundaries could be used to understand entropy production [9,10], the relationship between particles and energy [11], and thermodynamical paradoxes [12–14]. The DCE has the potential to be measured [15,16]. Indeed, one experiment claims to have effectively measured the DCE using a superconducting quantum interference device that acts as a moving mirror [17]. In another recent set of experiments [18], an analogue of the DCE has been observed in the case of a Bose-Einstein condensate.

One aspect of the moving mirror model that has been largely unexplored is the study of the time dependence of the particle production process. The time dependence of the stress-energy tensor for the quantized field has been worked out. However, the stress-energy contains vacuum polarization effects along with particle production effects, and in most cases there is no clear way of separating the two. In a flat-space background the Bogolubov transformation between the *in* and *out* vacuum states can be used to accurately describe the particle production process. However, the resulting particle frequency spectrum retains no information regarding the time dependence of creation.

One way to explore the time dependence of particle production is through the use of wave packets. Hawking [19] made use of such packets to describe the late-time behavior of black hole radiation when a black hole forms from collapse. In the context of a moving mirror, wave packets have been used by Dorca and Verdaguer [20] for a specific class of trajectories that generate a thermal spectrum at late times.

In this paper we explore the use of wave packets as a means of obtaining information about the time dependence of particle production due to accelerating mirrors in $(1 + 1)$ dimensions. We do so using two previously investigated trajectories and four new ones. In each case we compare the particle creation results with the stress energy of the quantum field. We work with a massless minimally coupled free scalar field. The packets are obtained by integrating the modes of the quantum field over specific frequency ranges using a parametrized weighting function that creates a packet whose amplitude is largest near a particular time that is related to the value of one of the parameters. By computing the Bogolubov transformation using packets for the modes in the *out* vacuum state, it is possible to obtain an expression for the number of particles produced in various frequency and time intervals as a function of time [21]. There is a fundamental uncertainty principle involved in working with the wave packets such that small frequency bins lead to good resolution in frequency and poor resolution in time, and vice versa. We explore the effects of this uncertainty relation for the trajectories chosen.

To facilitate the investigation, we have restricted our attention to mirror trajectories for which the Bogolubov components can be computed analytically. Only a small number of classes of trajectories has previously

*mgood@ntu.edu.sg
†anderson@wfu.edu
‡evans@physics.unc.edu

been considered for which it is possible to analytically compute the Bogolubov coefficients. These include the trajectories studied by Carlitz and Willey [7], which are designed so that there is a constant flux of energy, and the class of trajectories studied by Walker and Davies [22], which involve a mirror that starts at rest in the infinite past, accelerates, and ends at rest in the infinite future. In this paper we introduce four new trajectories for which the Bogolubov coefficients can be computed analytically. Three of these involve mirrors that start at rest in the infinite past. In one case the mirror trajectory is also asymptotically static in the future, in another the mirror's speed is asymptotically constant, and in the third the mirror's speed approaches the speed of light. In this third case, the trajectory nevertheless ends up at future timelike infinity instead of being asymptotic to a null trajectory. A fourth class of trajectories begins in the same way as those studied by Carlitz and Willey but then, instead of becoming asymptotic to a null ray at late times, approaches a constant velocity and thus becomes inertial.

In the only previous use of wave packets for the moving mirror model that we are aware of, Dorca and Verdaguer [20] studied the asymptotic form of the trajectory originally discussed by Davies and Fulling [2,3]. Their procedure involved wave packets for modes in both the *in* and *out* states. This technique allowed them to obtain a finite spectrum even though the total number of particles produced by the mirror in that model is infinite.

Here we use wave packets only on the modes that approach future null infinity to the right, $\mathcal{I}_R^+$, and are in the *out* vacuum state. The idea is to model what a particle detector at a large distance from the mirror would see. It turns out that one can compute either the packets first and then the Bogolubov transformation to determine the number of particles in a given packet, or one can do the computation in reverse order. We do the latter and first compute the exact Bogolubov transformation for the modes and integrate over frequencies using the appropriate weighting function [21] to obtain the Bogolubov coefficient for a packet. To obtain the total number of particles in the frequency range for that packet, we then integrate over the entire frequency range ω' of the modes in the *in* vacuum state. For two of the trajectories considered, there is an infrared divergence in the number of particles created, which manifests as a divergence in the number of particles in those packets that include modes of arbitrarily small frequencies. Any real detector would have an infrared cutoff, so we eliminate this divergence through the use of a low-frequency cutoff in the computation of the wave packets. That is, for these trajectories, we do not consider packets that include modes in the *out* state with arbitrarily small frequencies. In two other cases, the Bogolubov transformation results in an infrared divergence in the total number of particles created, but there is no corresponding divergence in the number of particles in the packets with small frequency modes. In the other two cases, there are no infrared divergences, and the total number of particles is finite.

The outline of this paper is as follows. In Sec. II we review the relevant aspects of the moving mirror model in $(1 + 1)$ dimensions in some detail. In Sec. III we discuss both the Carlitz-Willey [7] and Walker-Davies [22] trajectories. For the Carlitz-Willey trajectory, we first review some previous results and provide an analytic expression for the trajectory. We then use wave packets to show that the spectrum is time independent with a Planck character. We analytically compute the spectrum at a given time for wave packets of various frequency widths to investigate the distortion of the spectrum. For the Walker-Davies trajectory, we review some of the analytic results found previously. Unlike the Carlitz-Willey case, it does not appear possible to calculate analytically the expected number of particles in the wave packet modes. In Sec. IV we discuss four new trajectories and for each compute the relevant Bogolubov coefficients; the stress-energy tensor; the number of particles produced at a given frequency; and, for one trajectory, the total number of particles produced. Section V includes a comparison of the time dependence of the stress-energy tensor for the quantum field and the number of particles produced, where the latter is investigated through the use of wave packets. The difficulties encountered in obtaining simultaneously good time and frequency resolution for the number of particles produced are discussed, as well as the divergences that occur for some trajectories in the number of particles produced and the energy of those particles. Our conclusions are given in Sec. VI. Throughout this paper units are used such that $\hbar = c = 1$.

II. BACKGROUND

The moving mirror model in $(1 + 1)$ dimensions consists of a quantized massless scalar field in flat space that obeys Dirichlet boundary conditions on a perfectly reflecting (mirror) boundary. The scalar field satisfies the wave equation

$$\Box\Phi = 0. \tag{2.1}$$

In this paper we always expand the field in terms of mode functions that are parametrized by the frequency ω. Denoting them for the moment as ϕ_ω, they obey the equation

$$(-\partial_t^2 + \partial_x^2)\phi_\omega = -\partial_u\partial_v\phi_\omega = 0, \tag{2.2}$$

with

$$u \equiv t - x, \tag{2.3a}$$

$$v \equiv t + x. \tag{2.3b}$$

The general solution is

$$\phi_\omega = g(v) + h(u), \tag{2.4}$$

with g and h being arbitrary functions. The mode functions are normalized using the scalar product

$$(\phi_1, \phi_2) \equiv -i \int_\Sigma d\Sigma n^\mu [\phi_1(x) \overleftrightarrow{\partial}_\mu \phi_2^*(x)]. \tag{2.5}$$

Here Σ is any Cauchy surface for the spacetime, n^μ is a future-directed unit normal to that surface [21], and we adopt the usual notation for the derivative acting to the right first and then to the left with a minus sign [23]. For this scalar product, the canonical relations hold,

$$(\phi_\omega(x), \phi_{\omega'}(x)) = -(\phi_\omega^*(x), \phi_{\omega'}^*(x)) = \delta(\omega - \omega'), \tag{2.6a}$$

$$(\phi_\omega(x), \phi_{\omega'}^*(x)) = 0. \tag{2.6b}$$

For Minkowski space with no boundaries, we can choose the normalized modes

$$\phi_{\omega u} = \frac{1}{\sqrt{4\pi\omega}} e^{-i\omega u}, \tag{2.7a}$$

$$\phi_{\omega v} = \frac{1}{\sqrt{4\pi\omega}} e^{-i\omega v}. \tag{2.7b}$$

Then

$$\Phi = \int_0^\infty \frac{d\omega}{\sqrt{4\pi\omega}} [a_{\omega u} e^{-i\omega u} + a_{\omega v} e^{-i\omega v} + a_{\omega u}^\dagger e^{+i\omega u} + a_{\omega v}^\dagger e^{+i\omega v}], \tag{2.8}$$

with $a_{\omega u}$, $a_{\omega v}$, $a_{\omega u}^\dagger$, and $a_{\omega v}^\dagger$ being the usual annihilation and creation operators.

If there is a mirror with trajectory $z(t)$, so that at any time t the mirror is at the position $x = z(t)$, then the spacetime effectively has a boundary. In this paper we only consider solutions to the mode equation that are to the right of the mirror and incorporate reflection from the mirror's surface. We also only consider mirror trajectories that begin at past timelike infinity, i^-. In this case past null infinity, $\mathcal{I}^-$, only consists of the surface $u = -\infty$. This is a Cauchy surface. If the mirror trajectory ends at future timelike infinity, i^+, then future null infinity, $\mathcal{I}^+$, only consists of the surface $v = \infty$, and this is a Cauchy surface. But if the trajectory is asymptotic to the null ray $v = v_0$, then $\mathcal{I}^+$ has two parts, $\mathcal{I}_R^+$ and $\mathcal{I}_L^+$, using the notation of Ref. [7]. The surface $\mathcal{I}_R^+$ lies at $v = \infty$, and $\mathcal{I}_L^+$ consists of the part of the surface $u = \infty$ that goes from $v = v_0$ to $v = \infty$. Taken together they also provide a Cauchy surface.

It is useful to evaluate the scalar product (2.5) using the Cauchy surfaces for $\mathcal{I}^-$ and $\mathcal{I}^+$. It can be shown (see, e.g., Ref. [24]) that for $\mathcal{I}^-$

$$(\phi_1, \phi_2) = -i \int_{-\infty}^\infty [\phi_1(u = -\infty, v) \overleftrightarrow{\partial}_v \phi_2^*(u = -\infty, v)] dv, \tag{2.9}$$

and for $\mathcal{I}^+$

$$(\phi_1, \phi_2) = -i \int_{-\infty}^\infty [\phi_1(u, v = \infty) \overleftrightarrow{\partial}_u \phi_2^*(u, v = \infty)] du - i \int_{v_0}^\infty [\phi_1(u = \infty, v) \overleftrightarrow{\partial}_v \phi_2^*(u = \infty, v)] dv. \tag{2.10}$$

If Dirichlet boundary conditions are imposed on the scalar field, then the mode functions ϕ_ω must vanish at the location of the mirror. To quantify this, it is useful to introduce functions $u_m(t)$ and $v_m(t)$ that give the values of u and v at the location of the mirror at a given time t. Thus,

$$u = u_m(t) = t - z(t), \tag{2.11a}$$

$$v = v_m(t) = t + z(t). \tag{2.11b}$$

We can invert the first equation to get t via a function $t_m(u)$, or we can invert the second to get t via a function $\bar{t}_m(v)$.

In the presence of a mirror, we can consider either the mode functions that are positive frequency at $\mathcal{I}^-$, and thus correspond to the *in* vacuum state, or the mode functions that are positive frequency at $\mathcal{I}^+$, and thus correspond to the *out* vacuum state. The modes that are positive frequency at $\mathcal{I}^-$ are

$$\phi_{\omega'}^{\text{in}} = \frac{1}{\sqrt{4\pi\omega'}} [e^{-i\omega' v} - e^{-i\omega' p(u)}]. \tag{2.12}$$

Substitution into Eq. (2.6) using Eq. (2.9) shows that the normalization is correct. For these mode functions to vanish at the mirror we must have $v = p(u)$ *at the location of the mirror*. If we invert Eq. (2.11a) above to find $t = t_m(u)$ and then use the definition (2.11b), we find that

$$p(u) = t_m(u) + z(t_m(u)), \tag{2.13}$$

which fixes the function $p(u)$.

In a general left-right construction (for mirrors that have a horizon at v_0), there are two sets of mode functions that are positive frequency at $\mathcal{I}^+$. One set, which we will denote as ϕ_ω^R, is nonzero at $\mathcal{I}_R^+$ and zero at $\mathcal{I}_L^+$.[1] The other set, ϕ_ω^L, is zero at $\mathcal{I}_R^+$ and nonzero at $\mathcal{I}_L^+$. The former is given by

$$\phi_\omega^{\text{R,out}} = \frac{1}{\sqrt{4\pi\omega}} [e^{-i\omega f(v)} - e^{-i\omega u}], \quad v < v_0. \tag{2.14}$$

Mirrors that are asymptotically inertial in the future have $v_0 = \infty$. Note that all trajectories that begin at past timelike infinity, i^-, (the only type we consider here) span the range $-\infty < u < \infty$. Substitution into Eq. (2.6) using Eq. (2.10) shows that these modes are normalized correctly also. Again, for these modes to vanish at the mirror, we must have $u = f(v)$ *at the location of the mirror*, which is the inverse relation to $v = p(u)$ and an equivalent

[1]The left and right coefficient formulation lies at the crux of the calculations in Ref. [7], and, despite the call for more attention [25], the construction has been underused.

representation of the mirror trajectory in u, v coordinates. If Eq. (2.11b) is inverted to find $t = \bar{t}_m(v)$ and the definition (2.11a) is used, then one finds that

$$f(v) = \bar{t}_m(v) - z(\bar{t}_m(v)), \tag{2.15}$$

which fixes the function $f(v)$.

There are no other modes if $v_0 = \infty$. But if the mirror's trajectory is asymptotic to the null surface $v = v_0$, then one must also include the set of modes ϕ^L_ω that reach $\mathcal{I}^+_L$ and never interact with the mirror. Substituting into Eq. (2.6) and using Eq. (2.10), one finds that

$$(\phi^L_\omega, \phi^L_{\omega'}) = -i\int_{v_0}^{\infty} dv \phi^L_\omega \overleftrightarrow{\partial}_v \phi^{L*}_{\omega'} = \delta(\omega - \omega'). \tag{2.16}$$

To further examine the behavior of these modes, it is useful to work with a specific trajectory. This has been done by Carlitz and Willey [7] for a trajectory with a future horizon. We study other aspects of this trajectory in Sec. III.

The usual procedure for calculating interesting observable quantities, such as the energy or particle number, starts with the choice of an appropriate trajectory, $z(t)$. Then either the function $p(u)$ or its inverse $f(v)$ is found using the procedures described above. A key aspect of these procedures involves the solution of the relevant, and sometimes transcendental, function inversions. This requirement has made it difficult to find trajectories that allow both a fully analytic description of the mirror's motion and an analytic calculation of the associated Bogolubov coefficients (see below).

The function $p(u)$, commonly called the ray-tracing function [26], characterizes the mirror trajectory and is incorporated in the modes, the two-point function, the energy flux, and the correlation functions. The trajectories and, where known, the ray-tracing functions for the mirror trajectories considered in this paper are given in Table I.

A. Bogolubov transformations

One way to describe the particle production that arises in the presence of an accelerating mirror is to use the Bogolubov transformation. The positive frequency modes at $\mathcal{I}^-$, $\phi^{\text{in}}_{\omega'}$, form a complete set, and one can expand modes at $\mathcal{I}^+$ in terms of them,

$$\phi^J_\omega = \int_0^\infty d\omega' [\alpha^J_{\omega\omega'} \phi^{\text{in}}_{\omega'} + \beta^J_{\omega\omega'} \phi^{\text{in}*}_{\omega'}], \tag{2.17}$$

with J representing either R or L. Using the relations (2.6), one finds

$$\alpha^J_{\omega\omega'} = (\phi^J_\omega, \phi^{\text{in}}_{\omega'}), \tag{2.18a}$$
$$\beta^J_{\omega\omega'} = -(\phi^J_\omega, \phi^{\text{in}*}_{\omega'}). \tag{2.18b}$$

The field Φ expressed in terms of the mode functions can be represented in either of two ways:

$$\Phi = \int_0^\infty d\omega' [a^{\text{in}}_{\omega'} \phi^{\text{in}}_{\omega'} + a^{\text{in}\dagger}_{\omega'} \phi^{\text{in}*}_{\omega'}] \tag{2.19a}$$
$$= \sum_J \int_0^\infty d\omega [b^J_\omega \phi^J_\omega + b^{J\dagger}_\omega \phi^{J*}_\omega]. \tag{2.19b}$$

Using $b^J_\omega = (\Phi, \phi^J_\omega)$ [21] one finds

$$b^J_\omega = \int_0^\infty d\omega' [(\alpha^J_{\omega\omega'})^* a^{\text{in}}_{\omega'} - (\beta^J_{\omega\omega'})^* a^{\text{in}\dagger}_{\omega'}]. \tag{2.20}$$

If the field is in the *in* vacuum state specified by the positive frequency modes at $\mathcal{I}^-$, we can use the operator $N^J_\omega \equiv (b^J_\omega)^\dagger b^J_\omega$ to compute the average number of particles with frequency ω that reach $\mathcal{I}^+_J$,

$$\langle N^J_\omega \rangle \equiv \langle 0_{\text{in}} | N^J_\omega | 0_{\text{in}} \rangle = \int_0^\infty d\omega' |\beta^J_{\omega\omega'}|^2. \tag{2.21}$$

The expectation value of the total number of particles that reach $\mathcal{I}^+_J$ is

$$\langle N^J \rangle \equiv \langle 0_{\text{in}} | N^J | 0_{\text{in}} \rangle = \int_0^\infty d\omega \int_0^\infty d\omega' |\beta^J_{\omega\omega'}|^2. \tag{2.22}$$

Since we are primarily concerned with the number of particles that reach $\mathcal{I}^+_R$, we will focus on the computation of $\beta^R_{\omega\omega'}$. If the Cauchy surface $\mathcal{I}^-$ is used, then Eq. (2.18b) along with Eqs. (2.9), (2.12), and (2.14) give

TABLE I. Some classes of trajectories, $z(t)$, and the ray-tracing functions $p(u)$ and $f(v)$ associated with them.

	Trajectory	$p(u)$	$f(v)$
Static	$z = 0$	$p = u$	$f = v$
Constant velocity	$z = -v_0 t$	$p = \frac{1-v_0}{1+v_0} u$	$f = \frac{1+v_0}{1-v_0} v$
Uniform acceleration	$z = \kappa^{-1} - \sqrt{\kappa^{-2} + t^2}$	$p = \frac{u}{1+\kappa u}$	$f = \frac{v}{1-\kappa v}$
Carlitz-Willey	$z = -t - \frac{1}{\kappa} W(e^{-2\kappa t})$	$p = -\frac{1}{\kappa} e^{-\kappa u}$	$f = -\frac{1}{\kappa} \log(-\kappa v)$
Walker-Davies	$t = -z \pm A\sqrt{e^{-2z/B} - 1}$		
Arctx	$z = -\frac{1}{\mu} \tan^{-1}(e^{\mu t})$		
Darcx	$z = -\frac{\xi}{\nu} \sinh^{-1}(e^{\nu t})$		
Proex	$z = -\frac{1}{\rho} W(e^{\rho t})$	$p = u - \frac{1}{\rho} W(2e^{\rho u})$	$f = v + \frac{2}{\rho} e^{\rho v}$
Modified Carlitz-Willey	$z = -\frac{1-\sigma}{1+\sigma} t - W[e^{-2\kappa t}/(1+\sigma)]/\kappa$	$p = \sigma u - \frac{1}{\kappa} e^{-\kappa u}$	$f = \frac{v}{\sigma} + \frac{1}{\kappa} W(e^{-v\kappa/\sigma}/\sigma)$

$$\beta^R_{\omega\omega'} = \frac{1}{4\pi\sqrt{\omega\omega'}} \int_{-\infty}^{v_0} dv e^{-i\omega' v - i\omega f(v)} \left(\omega' - \omega \frac{df(v)}{dv}\right). \tag{2.23}$$

If the Cauchy surface $\mathcal{I}^+_R$ is used, then one similarly finds

$$\beta^R_{\omega\omega'} = \frac{1}{4\pi\sqrt{\omega\omega'}} \int_{-\infty}^{\infty} du e^{-i\omega u - i\omega' p(u)} \left(\omega' \frac{dp(u)}{du} - \omega\right). \tag{2.24}$$

These expressions are, of course, equivalent.

It is possible to write Eq. (2.24) in terms of a time integral over a function of the trajectory $z(t)$. Since $p(u)$ is a fixed function of u and u ranges from $-\infty$ to $+\infty$, one can substitute $u_m(t)$ for u in Eq. (2.24). Then using Eq. (2.11a) to change variables, one finds

$$\beta^R_{\omega\omega'} = \frac{1}{4\pi\sqrt{\omega\omega'}} \int_{-\infty}^{\infty} dt e^{-i\omega_+ t + i\omega_- z(t)} (\omega_+ \dot{z}(t) - \omega_-), \tag{2.25}$$

where $\omega_+ \equiv \omega + \omega'$ and $\omega_- \equiv \omega - \omega'$. This expression is applicable for trajectories that are asymptotically inertial in the limits $t \to \pm\infty$. Note that if we consider an inertial trajectory, it is easy to show that $\beta^R_{\omega\omega'} = 0$. Thus, as expected no particles are produced when the mirror does not accelerate.

It is not hard to show that the Bogolubov coefficient $\alpha_{\omega\omega'}$ may be obtained from the above expressions for $\beta_{\omega\omega'}$ by letting $\omega' \to -\omega'$ everywhere in the expressions for $\beta_{\omega\omega'}$, except for the factor $1/\sqrt{\omega\omega'}$, which must remain unchanged. Finally, we note that if the trajectory is initially inertial and the acceleration does not continue forever, then the total energy produced is finite and given by the following sum over the quantum modes [11]:

$$E_{qs} = \int_0^\infty \omega \langle N_\omega \rangle d\omega. \tag{2.26}$$

B. Stress-energy tensor

The renormalized stress-energy tensor for the massless, minimally coupled scalar field was computed in terms of the function $p(u)$ and in terms of the trajectory $z(t)$ by Davies and Fulling [2]. They found that the energy flux produced by the mirror as a function of u is given by[2]

$$\langle T_{uu} \rangle = \frac{1}{24\pi}\left[\frac{3}{2}\left(\frac{p''}{p'}\right)^2 - \frac{p'''}{p'}\right], \tag{2.27}$$

where primes indicate derivatives with respect to u. Their expression for the energy flux in terms of $z(t_m(u))$ is

$$\langle T_{uu} \rangle = \frac{\dddot{z}(\dot{z}^2 - 1) - 3\dot{z}\ddot{z}^2}{12\pi(\dot{z} - 1)^4(\dot{z} + 1)^2}\Bigg|_{t=t_m(u)}, \tag{2.28}$$

where the dots refer to derivatives with respect to t. Equation (2.28) is equivalent to Eq. (2.27) evaluated at the surface of the mirror. In either case, it is easy to show that for an inertial trajectory $\langle T_{uu} \rangle = 0$, as would be expected when the scalar field is in the vacuum state.

It is also possible to write Eq. (2.28) in terms of the time derivative of the proper acceleration:[3]

$$\alpha \equiv \ddot{z}/(1 - \dot{z}^2)^{3/2}. \tag{2.29}$$

The result is

$$\langle T_{uu} \rangle = -\frac{\dot{\alpha}}{12\pi} \frac{\sqrt{1 + \dot{z}}}{(1 - \dot{z})^{3/2}}. \tag{2.30}$$

The overall negative sign implies that on the right-hand side of the mirror, a flux of negative energy is given off if the change in acceleration of the mirror is toward the right, and a flux of positive energy is given off if the change in acceleration is toward the left.

For trajectories that are asymptotically inertial in the limits $t \to \pm\infty$, $p(u) \to c_1 u + c_0$ for some constants c_1 and c_0. For trajectories considered in this paper, a finite amount of energy reaches $\mathcal{I}^+_R$ (except for the Carlitz-Willey or modified Carlitz-Willey classes). Because the flux (2.27) is only a function of u and therefore does not fall off at $\mathcal{I}^+_R$, the total amount of energy E_{st} that reaches $\mathcal{I}^+_R$ can be obtained by integrating over u,

$$E_{st} = \int_{-\infty}^{\infty} \langle T_{uu} \rangle du. \tag{2.31}$$

Walker [11] has a proof that $E_{st} = E_{qs}$ provided that the mirror is asymptotically inertial in both the past and future, i.e., $\alpha(\pm\infty) = 0$, and the velocity *toward* $\mathcal{I}^+_R$ never reaches the speed of light, $\dot{z}(\pm\infty) \neq 1$. Substituting Eq. (2.27) into Eq. (2.31) and integrating by parts, one finds

$$E_{st} = \frac{1}{48\pi} \int_{-\infty}^{\infty} \left(\frac{p''}{p'}\right)^2 du, \tag{2.32}$$

so long as the surface terms with p''/p' vanish as $u \to \pm\infty$. The result can also be written in terms of a time integral over a function of the trajectory of the mirror by letting $u \to u_m(t)$, inverting Eq. (2.11a) to find $t = t_m(u)$ and then using Eq. (2.28). The result is

$$E_{st} = -\frac{1}{12\pi} \int_{-\infty}^{\infty} \dot{\alpha} \sqrt{\frac{1 + \dot{z}}{1 - \dot{z}}}\, dt. \tag{2.33}$$

Integrating by parts gives another expression:

$$E_{st} = \frac{1}{12\pi} \int_{-\infty}^{\infty} \alpha^2 (1 + \dot{z}) dt, = \frac{1}{12\pi} \int_{-\infty}^{\infty} \frac{\ddot{z}^2}{(1 + \dot{z})^2 (1 - \dot{z})^3} dt. \tag{2.34}$$

[2]Some other components are $\langle T^{tt} \rangle = \langle T^{tx} \rangle = \langle T^{xx} \rangle = \langle T_{uu} \rangle$.

[3]The proper acceleration is the acceleration in the instantaneous rest frame of the mirror. Note that the time derivative is in the inertial frame, not the rest frame of the mirror.

Notice that this last form masks the dependence on the time derivative of the proper acceleration.

C. Wave packets

Another way to investigate particle production is to use wave packets [19,21]. An advantage of this approach, as discussed in the Introduction, is that one can study the time-dependent aspects of particle production.

A wave packet, ϕ_{jn}, can be constructed from ϕ_ω by integrating over a finite range of frequencies with a particular weighting function so that [21]

$$\phi_{jn} \equiv \frac{1}{\sqrt{\epsilon}} \int_{j\epsilon}^{(j+1)\epsilon} d\omega e^{2\pi i\omega n/\epsilon} \phi_\omega. \tag{2.35}$$

Here n takes on integer values, and j takes on nonnegative integer values. Substituting Eq. (2.14) into Eq. (2.35) and noting that the first term does not contribute due to rapid oscillations in the limit $v \to \infty$, one can see that the integral is largest for values close to $u = 2\pi n/\epsilon$. It is clear from Eq. (2.35) that the value of j is related to the frequency of the modes in the packet with $(j + 1/2)\epsilon$ giving the frequency at the center of the range and ϵ giving the width of the range. When the weighting functions are applied to the modes $e^{-i\omega u}/\sqrt{4\pi\omega}$, the resulting wave packets form a complete and orthonormal set.

One can use the scalar product to construct the Bogolubov coefficients that correspond to the wave packets [21]. As mentioned previously, we are concerned in this paper with the particles that reach $\mathcal{I}_R^+$. In that case

$$\beta^R_{jn,\omega'} = -(\phi^R_{jn}, \phi^{\text{in}*}_{\omega'}). \tag{2.36}$$

It is possible to obtain these wave packet coefficients directly from the coefficients $\beta^R_{\omega\omega'}$ by using the same weighting, integrating over frequency, and interchanging the order of integration,

$$\beta^R_{jn,\omega'} = \frac{1}{\sqrt{\epsilon}} \int_{j\epsilon}^{(j+1)\epsilon} d\omega e^{2\pi i\omega n/\epsilon} \beta^R_{\omega\omega'}. \tag{2.37}$$

The average number of particles produced for given values of n and j is

$$\begin{aligned}\langle N^R_{jn}\rangle &= \int_0^\infty d\omega' |\beta^R_{jn,\omega'}|^2 \\ &= \int_0^\infty d\omega' \int_{j\epsilon}^{(j+1)\epsilon} \frac{d\omega_1}{\sqrt{\epsilon}} \\ &\quad \times \int_{j\epsilon}^{(j+1)\epsilon} \frac{d\omega_2}{\sqrt{\epsilon}} e^{2\pi i(\omega_1-\omega_2)n/\epsilon} \beta^R_{\omega_1\omega'} \beta^{R*}_{\omega_2\omega'}.\end{aligned} \tag{2.38}$$

This quantity gives the average number of particles that reach $\mathcal{I}_R^+$ in the frequency range $j\epsilon \le \omega \le (j+1)\epsilon$ and in the approximate time range $(2\pi n - \pi)/\epsilon \le u \le (2\pi n + \pi)/\epsilon$. It can be used to estimate the average number of particles that a detector would see in this frequency range if it was turned on during the above time period near an event centered at some x and some large v. Thus, computation of $\langle N_{jn}\rangle$ for a range of values of j and n allows one to construct the evolution of the spectrum of the produced particles in time (to the extent allowed by the uncertainty relation) as it would be seen by a series of particle detectors spread out over a line of constant but large v.

Note that one can also estimate the total energy of the particles produced by multiplying the number of particles in a given bin by the frequency at the center of that bin,

$$E_{ep} = \sum_{j,n} \left(j + \frac{1}{2}\right)\epsilon \langle N_{jn}\rangle. \tag{2.39}$$

This estimate of the energy can be compared to the energy of particles produced, E_{qs}, or the total stress-energy flux, E_{st}, to test the accuracy of the wave packet description of particle production.

III. TWO PREVIOUSLY STUDIED MIRROR TRAJECTORIES

In this section we examine two previously studied types of mirror trajectories. One of these, developed by Carlitz and Willey [7], consists of a trajectory that has a future horizon at $v = v_0 = 0$ but no past horizon. The trajectory is designed to yield a constant stress-energy flux. The functional form of the trajectory allows many quantities of interest to be computed analytically. The second type is the class of trajectories studied by Walker and Davies [22]. For these trajectories, the mirror begins and ends asymptotically at rest. Thus, the total number of particles produced is finite. In this case too, a number of quantities can be obtained analytically. For both of these types of trajectories, we have extended the analysis by using wave packets. For the Carlitz-Willey trajectory we use them to compute the spectrum of created particles and for the Walker-Davies class of trajectories we use them to investigate the time dependence of the particle creation.

A. Carlitz-Willey trajectory

In their paper [7] Carlitz and Willey point out that if the motion of the mirror is specified [in u and $v = p(u)$ coordinates] by taking the ray-tracing function to be

$$p(u) = -\frac{1}{\kappa} e^{-\kappa u}, \tag{3.1}$$

then a constant energy flux results. Substitution into Eq. (2.27) gives the energy flux in terms of the free parameter κ,

$$\langle T_{uu}\rangle = \frac{\kappa^2}{48\pi}. \tag{3.2}$$

An implicit functional form of the trajectory in t and $x = z(t)$ coordinates can be obtained by substituting Eq. (3.1) into Eq. (2.13),

$$t + z(t) = -\frac{1}{\kappa} e^{-\kappa t + \kappa z(t)}. \tag{3.3}$$

Carlitz and Willey did not provide the explicit functional form for $z(t)$. However, we find that it can be given as

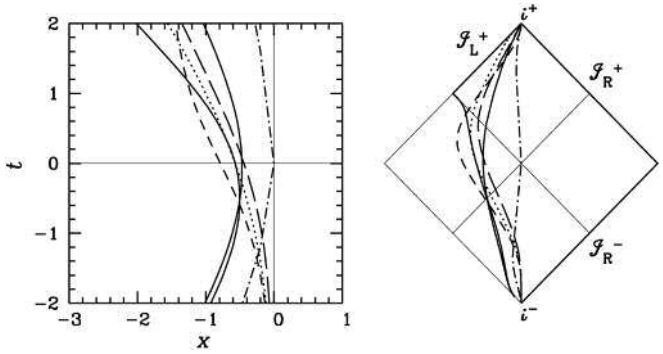

FIG. 1. Six analytically known mirror trajectories. In the left panel, the mirror trajectories are plotted in t and x coordinates. The right panel depicts the same trajectories in a Penrose diagram. The Carlitz-Willey trajectory, with $\kappa = 1$, and the modified Carlitz-Willey trajectory, with $\kappa = 1$ and $\sigma = 1/3$, are shown as solid curves. The Carlitz-Willey trajectory gives rise to a horizon at $v = 0$, while the modified Carlitz-Willey trajectory ends at future timelike infinity (i^+). The short-dashed curve indicates the Arctx mirror with $\mu = 1$, which is static in the distant past and future. The long-dashed curve is the Darcx trajectory with $\nu = 1$ and asymptotic future velocity $\xi = -1/2$. The Walker-Davies trajectory for $A = 2$, $B = 1$ is shown as the dotted-dashed curve. The Proex trajectory with $\rho = 1$ is denoted by the dotted curve. We consider only the region of spacetime to the right of a mirror. Thus, past null infinity on the left (not labeled) plays no role in our analysis. Similarly, there is an abbreviated portion of future null infinity on the left ($\mathcal{I}_L^+$), but only in the case of the Carlitz-Willey trajectory. All of the other mirror trajectories begin and end at i^- and i^+, respectively.

$$z(t) = -t - \frac{1}{\kappa} W(e^{-2\kappa t}), \tag{3.4}$$

which involves the Lambert W function (also known as the product logarithm). A plot of this trajectory is given in Ref. [7] and is shown also in our Fig. 1. It is not difficult to show that $\dot{z} \to \pm 1$ in the limits $t \to \mp\infty$ and that $z < 0$ for all time. The mirror trajectory begins at past timelike infinity, i^-, and at late times approaches $v = 0$. Substitution into Eq. (2.29) gives the proper acceleration,

$$\alpha(t) = -\frac{\kappa}{2\sqrt{W(e^{-2\kappa t})}}, \tag{3.5}$$

which is not constant, even though the energy flux is.

In Ref. [7] analytic expressions were found for the Bogolubov coefficients. In particular, it was found that[4]

$$\beta^R_{\omega\omega'} = \frac{1}{4\pi\sqrt{\omega\omega'}}\left\{-\frac{2\omega}{\kappa} e^{-\pi\omega/2\kappa}\left(\frac{\omega'}{\kappa}\right)^{-i\omega/\kappa}\Gamma\left[\frac{i\omega}{\kappa}\right]\right\}. \tag{3.6}$$

Thus,

$$|\beta^R_{\omega\omega'}|^2 = \frac{1}{2\pi\kappa\omega'}\frac{1}{e^{2\pi\omega/\kappa} - 1}, \tag{3.7}$$

resulting in both infrared and ultraviolet divergences for the quantity $\langle N^R_\omega \rangle$ in Eq. (2.21). This is not surprising given the fact that the acceleration of the mirror, while zero in the limit $t \to -\infty$, is nonzero at any finite time in the past. The radiation is produced with a thermal spectrum and propagates to $\mathcal{I}_R^+$ [7].[5]

It is possible to compute analytically the expectation value of the wave packet number $\langle N_{jn} \rangle$. First, substitute Eq. (3.6) into Eq. (2.38), interchange the order of integration, and make the variable transformation $y = \ln \omega'$. Then integrating over y gives a result that is proportional to $\delta(\omega_1 - \omega_2)$. Next integrating over ω_2 and setting $\omega_1 = \omega$ gives

$$\begin{aligned}\langle N_{jn} \rangle &= \frac{1}{\epsilon}\int_{j\epsilon}^{(j+1)\epsilon} d\omega \frac{1}{e^{2\pi\omega/\kappa} - 1} \\ &= \frac{\kappa}{2\pi\epsilon}\ln\left(\frac{e^{\frac{2\pi(j+1)\epsilon}{\kappa}} - 1}{e^{\frac{2\pi j\epsilon}{\kappa}} - 1}\right) - 1.\end{aligned} \tag{3.8}$$

There is a divergence in the particle count in the lowest frequency bin, $j = 0$. This result is similar to the infrared divergence found previously in $\langle N^R_\omega \rangle$, and the reason for it is the same. Physically, of course, one cannot measure particles of infinite wavelength. Thus, in a real particle detector, the lowest frequency bin would have a lower limit cutoff rather than extending all the way to $\omega = 0$.

It is also evident that for this mirror, there is no dependence in $\langle N_{jn} \rangle$ on the parameter n, and accordingly the average spectrum of particles recorded by a detector would be independent of time. This is almost certainly related to the fact that for this trajectory, the energy flux is constant.

To find effects of various frequency ranges ϵ on the spectrum and to recover the Planck form for the spectrum in the limit that $\epsilon \to 0$, one can first write the expression in Eq. (3.8) in terms of $\omega_j = (j + 1/2)\epsilon$ and then expand it in powers of ϵ with the quantity ω_j fixed. The result is

$$\begin{aligned}\langle N_{jn} \rangle = &\frac{1}{e^{2\pi\omega_j/\kappa} - 1} \\ &\times\left[1 + \frac{\pi^2 e^{2\pi\omega_j/\kappa}(1 + e^{2\pi\omega_j/\kappa})}{6\kappa^2(e^{2\pi\omega_j/\kappa} - 1)^2}\epsilon^2 + O(\epsilon^4)\right].\end{aligned} \tag{3.9}$$

With ϵ fixed, the second term approaches $\epsilon^2/(12\omega_j^2)$ for small ω_j and behaves like $\pi^2\epsilon^2/(6\kappa^2)$ for large values of ω_j. Thus, for a given frequency width, the deviation of the

[4]Here we have adapted the expression given in Ref. [7] to the conventions we are using.

[5]This thermal spectrum is, of course, that of a one-dimensional blackbody. A similar physical manifestation of one-dimensional thermal radiation is the resistor. Discovered by Nyquist [27] in 1928, a resistor in a lossless transmission line of great length in equilibrium at temperature T has thermal electric noise that is an analog of a blackbody in one dimension.

spectrum from the Planck form becomes more pronounced for smaller values of the central frequency ω_j.

B. Walker-Davies trajectory

The Walker-Davies trajectory [22] is given by the relation

$$t = -z \pm A\sqrt{e^{-2z/B} - 1}, \tag{3.10}$$

where $A > B$ and where the plus sign is adopted for $t > 0$ and the minus sign for $t < 0$. The trajectory is plotted in Fig. 1. Note that the curve is C^∞ in spite of the change in sign across branches for positive and negative values of t. The mirror begins at i^- at rest with t, $z = -\infty$. It accelerates to the right and then decelerates back to rest at $t = z = 0$. Then it first accelerates and then decelerates to the left, ending at rest at i^+ at $t = \infty$ and $z = -\infty$. The modes to the right of the mirror always end at $\mathcal{I}_R^+$. Therefore, we drop the subscript R in what follows.

Walker and Davies [22] calculated the stress tensor and found that[6]

$$\langle T_{uu}\rangle = \frac{B}{6\pi}\frac{(\chi^5 + \frac{1}{2}B\chi^4 - 2A^2\chi^3 - 3BA^2\chi^2 - 3A^4\chi - \frac{3}{2}A^4B)}{(\chi^2 + 2B\chi + A^2)^4}, \tag{3.11}$$

where χ is a parameter related to the null coordinate u by

$$u = B\ln(\chi^2/A^2 + 1) + \chi. \tag{3.12}$$

By integrating the flux over all u, they found the total energy to be

$$E_{st} = \frac{B^2}{48(A^2 - B^2)^{3/2}}. \tag{3.13}$$

They also were able to calculate the Bogolubov coefficients and found that

$$|\beta_{\omega\omega'}|^2 = \frac{2AB}{\pi^2}\left(\frac{\omega'}{\omega' + \omega}\right)\sinh(\pi\omega B)|K_q(r)|^2, \tag{3.14}$$

where $q \equiv -\frac{1}{2} + i\omega B$, $r \equiv A(\omega' + \omega)$, and $K_q(r)$ is a modified Bessel function of the second kind. We have not found an analytic expression for $\langle N_\omega\rangle$ in Eq. (2.21) and therefore also do not have one for E_{qs}. Furthermore, we do not have an analytic expression for $\langle N_{jn}\rangle$ in this case and instead have computed it numerically. We defer until Sec. V the discussion of these results.

IV. NEW TRAJECTORIES

In this section we consider four new types of trajectories for which it is possible to analytically compute the Bogolubov coefficients $\beta_{\omega\omega'}$. Having this analytic result in turn makes it feasible to compute numerically the expectation value of the particle number $\langle N_{jn}\rangle$ associated with the wave packets. Trajectories of each type are plotted in Fig. 1 for specific parameter choices. The functional form of the trajectories and their corresponding ray-tracing functions, where known, are summarized in Table I.

A. Arctx mirror trajectory

As seen in the previous section, the Walker and Davies [22] class is composed of trajectories that begin and end at rest in the limits $t \to \pm\infty$. They produce a finite number of particles and a finite amount of energy. Another trajectory with these features can be devised by taking

$$z(t) = -\frac{1}{\mu}\tan^{-1}(e^{\mu t}). \tag{4.1}$$

Here μ is a positive constant. Such a mirror starts at rest at $x = 0$ in the infinite past and ends at rest at $x = -\pi/2\mu$ in the infinite future. We refer to this trajectory as Arctx, drawn from "arctangent exponential."

The functional form of this trajectory is simple enough that a number of properties can be derived analytically. For example, the proper acceleration is given by

$$\alpha(t) = \mu\frac{4\,\mathrm{sech}(\mu t)\tanh(\mu t)}{[4 - \mathrm{sech}(\mu t)]^{3/2}}. \tag{4.2}$$

Starting from zero in the $t \to -\infty$ limit, the proper acceleration is negative for $t < 0$. It first increases and then decreases in magnitude, before reaching zero at $t = 0$. For positive values of t, it is positive and again first increases and then decreases to zero in the limit $t \to \infty$. A second important quantity, the stress energy, can also be obtained. Substitution of Eq. (4.1) into Eq. (2.28) gives

$$\langle T_{uu}\rangle = \frac{\mu^2\cosh[\mu t_m(u)](-5 - 2\cosh[2\mu t_m(u)] + \cosh[4\mu t_m(u)])}{3\pi(1 - 2\cosh[\mu t_m(u)])^2(1 + 2\cosh[\mu t_m(u)])^4}. \tag{4.3}$$

The finite total energy would follow from integrating this flux over u, but it is simpler to substitute Eq. (4.1) into Eq. (2.34) to find

[6]Note that there is a misprint in the numerator of their expression.

$$E_{st} = \frac{\mu}{2592\pi}(13\sqrt{3}\pi - 36). \tag{4.4}$$

Next it proves possible to calculate analytically the Bogolubov coefficients. Substituting Eq. (4.1) into Eq. (2.25), we find

$$\beta_{\omega\omega'} = g_0[g_1\Gamma(-m)\Gamma(-q) - g_2\Gamma(m)\Gamma(q)], \tag{4.5}$$

where

$$q \equiv \frac{i}{\mu}(\omega' + \omega), \tag{4.6a}$$

$$m \equiv \frac{1}{2\mu}(\omega' - \omega), \tag{4.6b}$$

$$g_0 \equiv ie^{\frac{i\pi q}{2}}\frac{\sqrt{4m^2+q^2}}{2\pi\mu}\frac{\sin(\pi m)}{\sin[\pi(m+q)]}, \tag{4.6c}$$

$$g_1 \equiv {}_2F_{1R}(1-m, 1-q, 1-m-q, -1)e^{-i\pi(m+q)}, \tag{4.6d}$$

$$g_2 \equiv {}_2F_{1R}(1+m, 1+q, 1+m+q, -1), \tag{4.6e}$$

and the ${}_2F_{1R}$ are regularized hypergeometric functions.

B. Darcx mirror trajectory

Another analytically simple set of trajectories is found by setting

$$z(t) = -\frac{\xi}{\nu}\sinh^{-1}(e^{\nu t}), \tag{4.7}$$

where ν and ξ are constants. To maintain future asymptotic inertial behavior, it is necessary that $0 < |\xi| < 1$. In this case the mirror begins at rest, and in the limit $t \to \infty$, its velocity approaches $-\xi$. We refer to this set of trajectories as Darcx, short for "drifting arc-hyperbolic sin of an exponential." A specific example is plotted in Fig. 1. Remarkably, the Bogolubov coefficients $\beta_{\omega\omega'}$ and other relevant quantities for these trajectories can also be calculated analytically. Since the process of deriving them is identical to that discussed previously, we simply collect the results in Table II.

C. Proex mirror trajectory

Another interesting trajectory that is asymptotically inertial in the past, $t \to -\infty$, can be defined using the Lambert W function,

$$z(t) = -\frac{1}{\rho}W(e^{\rho t}) = -t + \frac{1}{\rho}\ln W(e^{\rho t}) = \frac{1}{\rho}\ln[e^{-\rho t}W(e^{\rho t})], \tag{4.8}$$

where the equivalence between the expressions follows from the property $\ln W(z) = \ln z - W(z)$. We refer to this trajectory as Proex, which is short for "productlog exponential." A plot of its behavior is overlaid in Fig. 1. The late-time behavior of this trajectory is similar to the early time behavior of the Carlitz-Willey trajectory in that it approaches the speed of light at timelike infinity while not producing (in this case) a future horizon. The behavior is best seen in the Penrose diagram in the right panel of Fig. 1. Mathematically it can be seen by noting that as $x \to \infty$, $W(x) \to \infty$. Consequently, the value of v for the mirror at a given time, $v_m(t)$, has the behavior $v_m(t) \to \infty$ as $t \to \infty$. The velocity is

$$\dot{z}(t) = [1 + W(e^{\rho t})]^{-1} - 1, \tag{4.9}$$

which makes obvious the approach to light speed as $t \to \infty$. The proper acceleration,

$$\alpha(t) = -\rho\frac{W(e^{\rho t})}{[1 + 2W(e^{\rho t})]^{3/2}}, \tag{4.10}$$

is initially zero, increases with time until it reaches a maximum magnitude when the trajectory intersects the null ray $v = 0$, then decreases with time, vanishing in the limit $t \to \infty$.

For this trajectory both the ray-tracing function $p(u)$ and its inverse $f(v)$ can be computed analytically. The results are

$$p(u) = u - \frac{1}{\rho}W(2e^{\rho u}), \tag{4.11a}$$

$$f(v) = \frac{2}{\rho}e^{\rho v} + v. \tag{4.11b}$$

The Bogolubov coefficients $\beta_{\omega\omega'}$ can in turn be calculated analytically, as well as the energy flux. We summarize these and some other quantities in Table III.

D. Modified Carlitz-Willey trajectory

The final class of trajectories that we consider is a modification of the Carlitz-Willey trajectory. A term is

TABLE II. Bogolubov coefficients and other useful information for the Darcx trajectories.

Bogolubov coefficient with $b_+ \equiv b\omega + a\omega'$, $a_+ \equiv a\omega + b\omega'$, $\omega_+ \equiv \frac{1}{\nu}(\omega + \omega')$, $a \equiv \frac{1}{2\nu}(1+\xi)$, and $b \equiv \frac{1}{2\nu}(1-\xi)$.	$\beta_{\omega\omega'} = \frac{1}{4\pi\sqrt{\omega\omega'}}[-2^{i\omega_+}\frac{\xi}{\nu^2}\frac{2\omega'\omega}{b_+}\frac{\Gamma(-i\omega_+)\Gamma(ia_+)}{\Gamma(-ib_+)}]$
	$\lvert\beta_{\omega\omega'}\rvert^2 = \frac{\xi^2}{4\pi\nu^4}\frac{\omega'\omega}{\omega_+ a_+ b_+}\frac{\operatorname{csch}(\pi\omega_+)\operatorname{csch}(\pi a_+)}{\operatorname{csch}(\pi b_+)}$
Proper acceleration	$\alpha(t) = -\frac{\nu\xi e^{\nu t}}{[1-(\xi^2-1)e^{2\nu t}]^{3/2}}$.
Energy flux	$\langle T_{uu}\rangle = \frac{\nu^2}{12\pi}\frac{\xi\sqrt{e^{2\nu t_m(u)}+1}e^{\nu t_m(u)}[2(\xi^2-1)e^{2\nu t_m(u)}+1]}{(\sqrt{e^{2\nu t_m(u)}+1}+1+\xi e^{\nu t_m(u)})^2[(\xi^2-1)e^{2\nu t_m(u)}-1]^2}$.
Total energy	$E_{st} = \frac{\nu}{96\pi}(\frac{3+\xi^2}{2\xi^2}\ln\frac{1+\xi}{1-\xi} - \frac{3+\xi(3+2\xi)}{\xi(1+\xi)})$.

TABLE III. Bogolubov coefficients and other analytically derived information for the Proex trajectory.

Bogolubov coefficient	$\beta_{\omega\omega'} = \frac{1}{4\pi\sqrt{\omega\omega'}}(\frac{2\omega'}{\rho})(\frac{2\omega}{\rho})^{i(\omega+\omega')/\rho} e^{-\pi(\omega+\omega')/(2\rho)}\Gamma(-i(\omega+\omega')/\rho)$
	$\lvert\beta_{\omega\omega'}\rvert^2 = \frac{\omega'}{2\pi\omega\rho(\omega+\omega')}\frac{1}{e^{2\pi(\omega+\omega')/\rho}-1}$
Proper acceleration	$\alpha(t) = -\rho\frac{W(e^{\rho t})}{[1+2W(e^{\rho t})]^{3/2}}$
Spectrum of produced particles[a]	$\langle N_\omega\rangle = -\frac{1}{4\pi^2\omega}\ln(1-e^{-2\pi\omega/\rho}) - \frac{1}{2\pi\rho}\sum_{m=1}^{\infty}\Gamma(0, 2\pi\omega m/\rho)$
Energy flux	$\langle T_{uu}\rangle = \frac{\rho^2}{48\pi}\frac{[2-W(2e^{\rho u})]W(2e^{\rho u})}{[1+W(2e^{\rho u})]^4}.$
Total energy	$E_{st} = \frac{\rho}{96\pi}$

[a]Here $\Gamma(0, 2\pi\omega m/\rho)$ is an upper incomplete gamma function.

TABLE IV. Bogolubov coefficients and other useful information for the modified Carlitz-Willey class of trajectories.

Bogolubov coefficient	$\beta_{\omega\omega'} = -\frac{1}{2\kappa\pi}\sqrt{\frac{\omega}{\omega'}}e^{-\pi(\omega+\sigma\omega')/(2\kappa)}(\frac{\omega'}{\kappa})^{-i(\omega+\sigma\omega')/\kappa}\Gamma[i(\omega+\sigma\omega')/\kappa]$
	$\lvert\beta_{\omega\omega'}\rvert^2 = \frac{\omega}{2\pi\kappa\omega'(\omega+\sigma\omega')}\frac{1}{e^{2\pi(\omega+\sigma\omega')/\kappa}-1}$
Proper acceleration	$\alpha(t) = \frac{\kappa(1+\sigma)W(e^{-2\kappa t/(1+\sigma)}/(1+\sigma))}{2[\sigma+(1+\sigma)W(e^{-2\kappa t/(1+\sigma)}/(1+\sigma))]^{3/2}}$
Energy flux	$\langle T_{uu}\rangle = \frac{\kappa^2}{48\pi}\frac{1-2\sigma e^{\kappa u}}{(\sigma e^{\kappa u}+1)^2}.$

added that takes the acceleration to zero at late times. This causes the trajectory to become inertial in the future rather than asymptotically null. The final velocity is a free parameter. The trajectories are

$$z = -\frac{1-\sigma}{1+\sigma}t - \frac{1}{\kappa}W\left(\frac{e^{-2\kappa t/(1+\sigma)}}{1+\sigma}\right), \qquad (4.12)$$

with $0 \le \sigma \le 1$. A particular example is shown in Fig. 1 where one can see the divergence from the Carlitz-Willey trajectory at late times. For $\sigma = 0$ the trajectory reduces to the Carlitz-Willey one (3.4). As before with the other new trajectories, it proves possible to calculate the Bogolubov coefficients $\beta_{\omega\omega'}$ analytically, as well as a set of other relevant quantities. These are displayed in Table IV.

V. ANALYSIS OF ENERGY AND PARTICLE PRODUCTION

For each of the mirror trajectories we consider in this paper, the renormalized stress energy for the scalar field is known analytically and can be easily evaluated. Except for the Carlitz-Willey trajectory, the expectation value of the number of particles in a wave packet, $\langle N_{jn}\rangle$, cannot be calculated analytically, and we instead evaluate this quantity numerically. To do so accurately, however, it proved important to have analytic expressions for the Bogulobov coefficients $\beta_{\omega\omega'}$. The wave packets in turn provide a means of examining the time and frequency dependence of the created particles.

A. Time dependence

The correlation (or lack of it) between the number of particles produced at a given time and the energy flux $\langle T_{uu}\rangle$ differs markedly from one type of trajectory to the other. Because the mirror is in flat space, the Bogolubov transformation between the *in* and *out* vacuum states tells us about the average number of particles produced in an ensemble of identical systems. The energy flux given by the quantity $\langle T_{uu}\rangle$ gives information about the average flux of energy produced by the mirror as it accelerates. The energy flux is due to a combination of particle production and vacuum polarization effects.

In Fig. 2 the energy flux is shown for the various trajectories considered in this paper. From Eq. (2.30) one

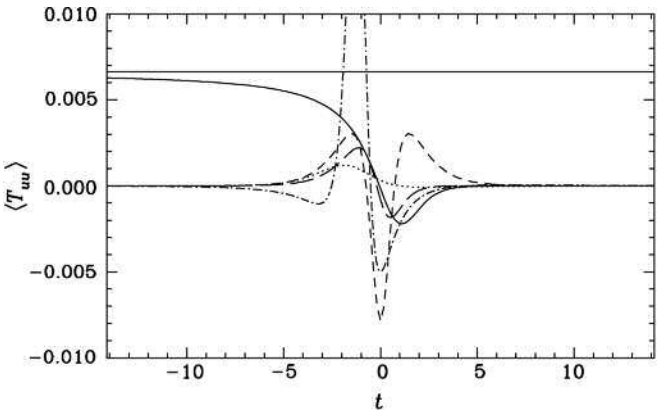

FIG. 2. The energy flux $\langle T_{uu}\rangle$ vs time is plotted for the various mirror trajectories. The parameters κ, μ, ν, and ρ have all been set equal to 1. For the Darcx trajectory, the value $\xi = 1/2$ was chosen, and for the modified Carlitz-Willey trajectory, $\sigma = 1/3$ was chosen. For the Walker-Davies trajectory, $A = 2$ and $B = 1$ were chosen. The energy flux in the Carlitz-Willey case is the constant solid line. The energy flux associated with the modified Carlitz-Willey trajectory is the solid curve, which coincides with the Carlitz-Willey value at early times but then diverges, briefly resulting in a burst of negative energy before decaying to zero. The flux associated with the Arctx trajectory is shown as the short-dashed curve, and that of the Darcx trajectory is indicated by the long-dashed curve. The flux from the Proex trajectory is depicted by the dotted curve and that of the Walker-Davies case by the dotted-dashed curve.

can see that the sign of the flux is closely tied with the change in the proper acceleration of the mirror. In particular as mentioned in Sec. II, the flux is negative if the change in the proper acceleration is toward the right and positive otherwise.

Figures 3 and 4 show the expectation value of the number of particles produced $\langle N_{jn}\rangle$ as a function of the time parameter n for the various trajectories we consider. In Fig. 3 the frequency parameter j is set to one because of infrared divergences that occur in N_{0n} for the Carlitz-Willey and modified Carlitz-Willey trajectories. For the trajectories in Fig. 4, j is set to zero because no such divergences occur. The packets, of course, sample the particle production discretely. We draw attention also to the small level of particle excitation that occurs for $j = 1$ in Fig. 3 as compared to that which occurs for $j = 0$ in Fig. 4. We return to this issue in Sec. V C.

There is a correlation between the number of particles created during a given time period and the flux of energy that occurs at that time for the Carlitz-Willey trajectory in Fig. 3 due to the fact that, as discussed in Sec. III A, the flux is constant in time and the number of particles $\langle N_{jn}\rangle$ is independent of the value of the time parameter n. As can be seen in Figs. 2 and 3, a correlation also occurs for the modified Carlitz-Willey trajectory at early times. However, the direct correlation is destroyed by the existence of a negative flux of energy after the time $t = 0$ when the trajectory has deviated significantly from the original Carlitz-Willey trajectory.

For the trajectories in Fig. 4, there is no direct correlation between the energy flux and the number of particles created. In fact for the Arctx trajectory, there is something of an anticorrelation in that at about the time of peak particle production, the flux is negative and has its greatest

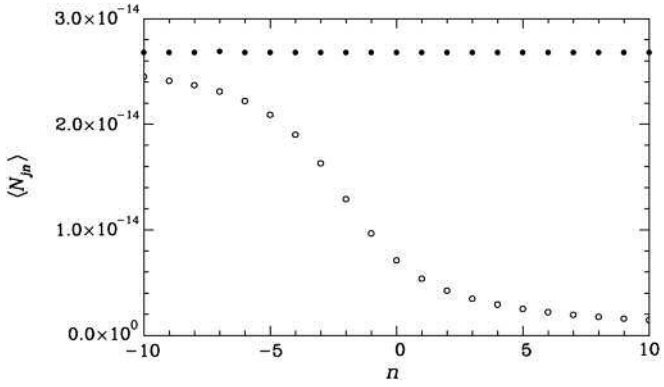

FIG. 3. The particle number as measured by wave packets, $\langle N_{jn}\rangle$, is plotted as a function of the packet time parameter n for the Carlitz-Willey (filled circles) and modified Carlitz-Willey (open circles) trajectories. In both cases the packet frequency width parameter ϵ has been set to $\sqrt{2}\pi$, and the first nondivergent frequency bin, $j = 1$, is shown. The parameter κ has been set to one, and for the modified Carlitz-Willey trajectory, we have taken $\sigma = 1/3$.

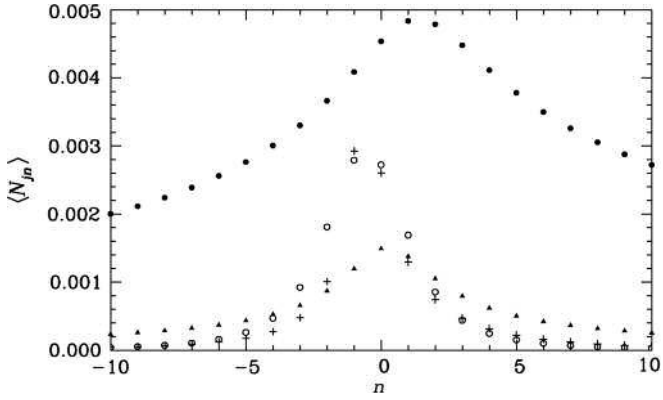

FIG. 4. The particle number as measured by wave packets, $\langle N_{jn}\rangle$, is plotted as a function of the packet time parameter n. In each case the packet frequency width parameter ϵ has been set to $\sqrt{2}\pi$, and the lowest frequency bin $j = 0$ is shown. The parameters μ, ν, and ρ have all been set to one. For the Darcx trajectory, the value $\xi = 1/2$ was chosen, and for the Walker-Davies case, $A = 2$ and $B = 1$ were chosen. The value of N_{0n} is denoted by the open circles for the Arctx trajectory, the triangles for the Darcx trajectory, the filled circles for the Proex trajectory, and the pluses for the Walker-Davies trajectory.

magnitude. This shows clearly the limitations in using the stress-energy tensor to describe the number of particles created. Because of vacuum polarization effects, which can include fluxes of negative energy, it is virtually impossible to separate out the contribution from the created particles.

B. Frequency spectrum and simultaneous frequency and time resolution

Wave packets can also be used to measure the frequency spectrum of the created particles. Good frequency resolution is obtained by choosing a small value for ϵ. As an example consider Fig. 5 for the Arctx trajectory with a wave packet frequency width parameter $\epsilon = 0.01$. The spectrum is a function of the packet index j, and we have set $n = 0$. Clearly good frequency resolution is obtained.

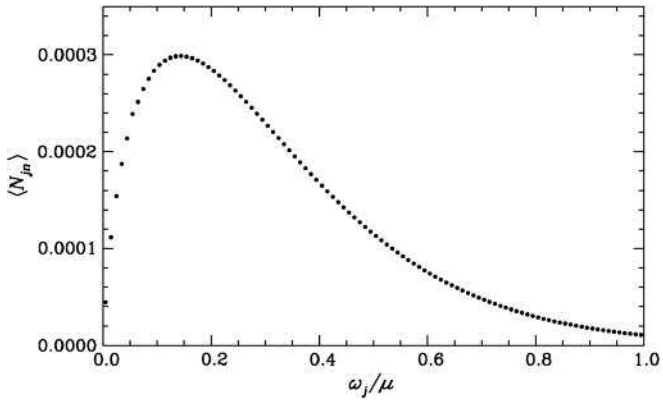

FIG. 5. The particle number as measured by wave packets, $\langle N_{jn}\rangle$, is plotted as a function of the packet frequency parameter j, with $n = 0$ and $\epsilon = 0.01$ for the Arctx trajectory.

In principle, the wave packet formalism allows particle production to be simultaneously resolved, within limits, in both frequency and time. The limits, of course, are set by the uncertainty relation. For any chosen ϵ, the wave packets have a width in frequency $\Delta\omega = \epsilon$ and an effective gating interval (width of time over which the particle detector is on) of $\Delta t \simeq 2\pi/\epsilon$. Thus, the time-bandwidth product (for these packets) is 2π. It may be possible to resolve time-dependent spectra for a process with sufficiently copious particle creation and for which changes in its spectrum occur over a long enough time interval. However, for the trajectories studied in this paper, it has not been possible to resolve the creation process in frequency and time simultaneously, such that a significant number of particles is found in many frequency and time bins. Some of the mirror trajectories have confined periods during which the acceleration peaks and is strong (i.e., Walker-Davies, Arctx, Darcx, and Proex). For these trajectories, when we choose a relatively small value of ϵ to provide good frequency resolution, we find the vast majority of the particles are created in the time bin $n = 0$. In contrast, when we choose a relatively large value of ϵ to gain good time resolution, we find that almost all of the particles reside in the lowest frequency bin, $j = 0$. Furthermore, it is not even possible to find some intermediate value of ϵ for which some time and frequency resolution is possible. Instead, in picking such an intermediate value of ϵ, we find that the vast majority of particles lie in the single bin with $n = j = 0$.

A different behavior occurs for the Carlitz-Willey trajectory. In this case a small ϵ will provide adequate frequency resolution, and yet not all of the particle creation occurs in a single time bin, such as $n = 0$. However, we have not really succeeded in simultaneous time and frequency resolution, since the Carlitz-Willey mirror gives a spectrum that is completely time independent. This then brings us to the modified Carlitz-Willey trajectory. The energy flux in this case is asymptotically constant in the distant past, but then at some point, the energy flux drops toward zero as the acceleration falls off, and the mirror becomes inertial. The particle creation behaves similarly. One might hope that this trajectory would result in a creation process that could be simultaneously resolved in frequency and time. However, here, too, we find that the acceleration falls off sufficiently rapidly that the transition from creation to effectively no creation occurs within one time bin (assuming ϵ has been set to allow good frequency resolution, i.e., many frequency bins within the transition or characteristic frequency $\omega_c \sim \kappa$).

To see what seems to be happening, consider the Arctx trajectory. In that case the parameter μ is dimensionally the inverse of time and ought to represent a characteristic frequency ω_c. In fact, as Fig. 5 shows, we find the peak of the particle creation spectrum is $\omega_c \simeq 0.14\mu$. However, the period τ of significant acceleration also depends on μ and is roughly $\tau \simeq \mu^{-1}$. The frequency and time scales are thus related by a single parameter. A related factor is that the expectation value of the total number of particles created $\langle N \rangle$ is a fraction of unity. In other words, in an ensemble of identically accelerated mirrors, in many cases there will be no particles produced at all. Similar time scale and frequency scale issues occur with the Darcx, Proex, and Walker-Davies trajectories.

We speculate that a trajectory might be crafted with two parameters: an acceleration scale μ, with $\tau \simeq \mu^{-1}$, and a duration of acceleration T, which satisfies $T \gg \tau$. For such a trajectory, enough particles may be created for a long enough period to allow a significant number of particles to be found in many time and frequency bins, giving good resolution. A mirror of this sort would undergo a large change in Lorentz factor over a time $\sim T$, and it would appear, over that time interval, like a mirror that is approaching a null horizon. We have not been able so far to find a trajectory with these properties for which the Bogolubov coefficients can be calculated analytically.

The challenge of finding significant wave packet excitation that is simultaneously spread across a range of both time and frequency bins may also lie in the inherent nature of the time-bandwidth product of our orthonormal wave packets. The time-bandwidth product of these packets is 2π, while the fundamental limit of the uncertainty principle is $1/2$. This may be a contribution to nonuniformity in the creation spectra, since by their construction, these orthonormal wave packets are unable to reach the limits of the uncertainty principle.

The fact that it is not possible to obtain significant particle creation in simultaneous bins of both frequency and time for the trajectories considered may have interesting experimental consequences if a system that was in some way like one of these trajectories could be studied in the laboratory. However, the relatively small amount of particle production that occurs might make this very difficult.

C. Total number of particles produced and their energy

In Sec. II expressions were given that allow one to compute the total number of particles produced and their total energy. With some mirror trajectories, we have found one or both of these quantities to be divergent.

To compute the total number of particles produced, one can use Eq. (2.22), and to compute their total energy, one can use either Eq. (2.26) or Eq. (2.31). Comparison of Eqs. (2.21), (2.22), and (2.26) shows that it is possible to have a divergent number of particles produced and yet have a finite total energy, provided that the divergence in the number of particles is due to an infrared divergence in N_ω and that it is not too strong.

Substitution of $|\beta_{\omega\omega'}|^2$ into Eqs. (2.22) and (2.26) for the Walker-Davies and Arctx trajectories results in both a finite number of particles produced and a finite total energy for those particles. We have evaluated $\langle N \rangle$ numerically for

both trajectories. For the Walker-Davies trajectory, $\langle N\rangle$ depends on the ratio $0 < B/A < 1$. As an example, for $B/A = 1/2$ we find $\langle N\rangle \approx 0.0121$. For the Arctx trajectory, $\langle N\rangle$ is independent of the value of the parameter μ as can easily be seen by substituting Eq. (4.5) into Eq. (2.22) and making variable changes of the form $\omega = \mu x$. We find $\langle N\rangle \approx 0.0134$. An interesting point is that both of these values are small compared to unity. Thus, in an ensemble of identical systems, in most cases there would be no excitation of any mode, and no particles would be produced. The total energy produced for the Walker-Davies trajectory was computed by them and is given in Eq. (3.13). For the Arctx trajectory, it is given in Eq. (4.4). As discussed in Sec. II, the energies E_{st} in Eq. (2.31) and E_{qs} in Eq. (2.26) are the same. This can be used as a check on the computations of the Bogolubov coefficients $\beta_{\omega\omega'}$. We have computed E_{qs} numerically (in specific cases for the Walker-Davies trajectories and in general for Arctx) and found the values to be equal to those for E_{st}.

For the other classes of trajectories besides Arctx and Walker-Davies, the number of particles $\langle N\rangle$ diverges. For the Proex trajectory, we have computed $\langle N_\omega\rangle$ analytically. Examination of the result, which is shown in Table III, indicates an infrared divergence of the form

$$\langle N_\omega\rangle \sim -\frac{\ln(2\pi\omega/\rho)}{\omega}. \tag{5.1}$$

This behavior results in a divergence in the total number of particles $\langle N\rangle$. However, when computing E_{qs} in Eq. (2.26), one multiplies $\langle N_\omega\rangle$ by a factor of ω before integrating over ω. The result is a finite value for E_{qs}. We have computed E_{qs} numerically and found agreement with the expression for E_{st}, which is given in Table III.

For the Darcx class of trajectories when ω is small, one can divide the integral in Eq. (2.21) into two parts, one with an integral from 0 to $\nu\lambda$ and a second integral from $\nu\lambda$ to ∞ with $1 \gg \lambda \gg \omega/\nu$. In the first integral, one can evaluate $|\beta_{\omega\omega'}|^2$ in the limit that both ω/ν and ω'/ν are small. The result is a contribution to $\langle N_\omega\rangle$ that is proportional to $1/\omega$. In the second integral, $\omega \ll \omega'$, and it is not hard to show that the integral is finite in the limit $\omega \to 0$. Thus, as with the Proex class of trajectories, we find that $\langle N\rangle$ is infinite, but E_{qs} is finite. We have numerically computed E_{qs} for specific values of the parameter ξ and shown that its value is the same as that for E_{st}, which is given in Table II.

For the Carlitz-Willey trajectory, one can see from the form of $|\beta_{\omega\omega'}|^2$ that there is both an infrared and ultraviolet divergence in the integral over ω' in Eq. (2.21). Thus, there is a divergence in both the particle number and the energy of the produced particles. The latter is trivially apparent from the constant flux of energy which occurs for these trajectories. For the modified Carlitz-Willey class of trajectories, one can see from the form of $|\beta_{\omega\omega'}|^2$ in Table IV that there is still the infrared divergence but no ultraviolet divergence when computing $\langle N_\omega\rangle$. The infrared divergence is strong enough to make $\langle N_\omega\rangle$ divergent for all values of ω.

One might ask what effect the packets have on those trajectories with infrared divergences. For the Carlitz-Willey trajectory, we were able to analytically compute the packets, and as seen in Eq. (3.8), there is a divergence for the packets with the lowest frequency range, $j = 0$. However, for all other packets, $\langle N_{jn}\rangle$ is finite, so the divergences are not nearly as strong as for $\langle N_\omega\rangle$.

For the modified Carlitz-Willey class of trajectories, there is also a divergence for packets with $j = 0$ but not for those with $j > 0$. To see this, one can divide the integral in Eq. (2.38) into two parts such that $I_1 = \int_0^{\kappa\lambda} d\omega'$ and $I_2 = \int_{\kappa\lambda}^{\infty} d\omega'$, with $0 < \lambda \ll 1$. For the second integral, which contains only nonzero values of ω', it is not difficult to see that for $\beta_{jn,\omega'}$ in Eq. (2.37), there are no infrared divergences resulting from the integral over ω. It can also be seen that $\beta_{jn,\omega'}$ is well enough behaved in the limit $\omega' \to \infty$ that there are no ultraviolet divergences so long as $\sigma > 0$. For the first integral, the value of ω'/κ is small. Here it is necessary to break the discussion into the cases $j = 0$ and $j > 0$. For $j > 0$ we take a small enough value of λ so that $\epsilon > \omega'$ for all values of ω' in the first integral. Then one can expand the function $\Gamma[i(\omega + \sigma\omega')/\kappa]$ in the expression for $\beta_{\omega\omega'}$ in Table IV in powers of ω'/ω. Keeping the leading-order term, one finds that

$$|\beta_{jn,\omega'}| \approx \frac{1}{2\pi\kappa\sqrt{\omega'\epsilon}}\left|\int_{j\epsilon}^{(j+1)\epsilon} d\omega\sqrt{\omega}\,e^{[2\pi i n/\epsilon - \pi/(2\kappa)]\omega} \times e^{-i(\omega/\kappa)\ln(\omega'/\kappa)}\Gamma(i\omega/\kappa)\right|. \tag{5.2}$$

By repeatedly integrating by parts, one can obtain a series in inverse powers of $\ln(\omega'/\kappa)$. Substituting into I_1 then shows that, to leading order, the integrand goes like $1/[\omega'(\ln(\omega'/\kappa))^2]$, which when integrated gives no divergence in the limit $\omega' \to 0$.

For $j = 0$ the situation is different. Here one can divide the absolute value of the integral in Eq. (2.37) into two parts, $J_1 = \int_0^{\kappa\lambda_1} d\omega$ and $J_2 = \int_{\kappa\lambda_1}^{\epsilon} d\omega$. The analysis for the second integral is exactly the same as for the case $j > 0$ with $\epsilon > \kappa\lambda_1$ and $1 \gg \lambda_1 \gg \lambda > 0$. For the first integral, we choose λ_1 to be small enough so that $|2\pi\kappa n/\epsilon - \pi/2|\lambda_1 \ll 1$. Then both ω/κ and ω'/κ are small, and

$$J_1 \approx \frac{1}{2\pi\kappa\sqrt{\omega'\epsilon}}\left|\int_0^{\kappa\lambda_1} d\omega\sqrt{\omega}\,e^{-i(\omega/\kappa)\ln(\omega'/\kappa)}\frac{\kappa}{\omega + \sigma\omega'}\right|. \tag{5.3}$$

Making the change of variable $z = -(\omega/\kappa)\ln(\omega'/\kappa)$, the upper limit becomes $-\lambda_1\ln(\omega'/\kappa)$, which for fixed λ_1 goes to infinity in the limit $\omega' \to 0$. The resulting integral can be computed analytically in terms of Fresnel integrals. The result to leading order in ω' is $J_1 \sim 1/\sqrt{-\omega'\ln(\omega'/\kappa)}$. This gives a contribution to I_1 that

when integrated results in a divergence at the lower limit $\omega' = 0$ and thus a divergence in $\langle N_{jn}\rangle$ for $j = 0$.

For the Darcx and Proex trajectories, it turns out there is no infrared divergence in $\langle N_{jn}\rangle$ even for $j = 0$ and even though $\langle N_\omega\rangle$ diverges in the limit $\omega \to 0$. This can be shown by bounding $\langle N_{jn}\rangle$ by computing the absolute values of each factor in the integrand of Eq. (2.38). The result is

$$\langle N_{jn}\rangle \le \frac{1}{\epsilon}\int_0^\infty d\omega'\left(\int_{j\epsilon}^{(j+1)\epsilon} d\omega|\beta_{\omega\omega'}|\right)^2. \quad (5.4)$$

It is not hard to show that for small ω', the integrand is finite in the limit $\omega' \to 0$ if $j > 0$ for both trajectories. If $j = 0$ then it is useful to again divide the integral over ω into two parts as was done above, except with $\kappa \to \nu$ and ρ, respectively, for the Darcx and Proex trajectories. Then as before the analysis for J_2 is the same as for $j > 0$. For J_1 both ω and ω' are small, making it possible to expand the terms in $|\beta_{\omega\omega'}|$. When this is done and the integral over ω is computed for the leading-order terms, we find that the result is finite in the limit $\omega' \to 0$ for the Darcx trajectories. For the Proex trajectory, we find that to leading order, $J_1 \sim \ln\omega'$ so that the integrand for the integral over ω' goes like $(\ln\omega')^2$, and a finite contribution is made to $\langle N_{0n}\rangle$.

As discussed in Sec. II, one can obtain an estimate of the energy of the created particles using the packet formalism by multiplying $\langle N_{jn}\rangle$ by the frequency in the middle of the range for each packet and summing over j and n as in Eq. (2.39). The resulting energy, E_{ep}, has been computed for the Arctx trajectory for two different values of ϵ. For the case shown in Fig. 5 with $\epsilon = 0.01$, the results agreed with E_{st} in Eq. (4.4) to within about 0.01%. In a separate calculation, with $\epsilon = 10$, the agreement was at the 1% level, which is remarkably good given the poor frequency resolution, which might be expected to drastically skew the energy summation.

For the Darcx class of trajectories with $\xi = 0.99$, $\sigma = 1$, and $\epsilon = 0.001$, we find agreement with the values of E_{st} to within four digits. The result was obtained by summing packets with $n = 0$ and values of j ranging from $j = 0$ to $j = 1175$.

For the Proex trajectory with $\rho = 1$, a numerical computation of E_{ep} for $\epsilon = 5 \times 10^{-5}$ gave results in agreement with E_{st} to approximately 0.08%. Energy packets with $n = 0$ and with a sum from $j = 0$ to $j = 12000$ were used in that calculation.

VI. CONCLUSION

We have investigated the particle production and the energy flux that result from a massless, minimally coupled scalar field in a two-dimensional flat space that contains an accelerating mirror. Dirichlet boundary conditions are assumed at the mirror and the field is assumed to be in the *in* vacuum state. Six different types of trajectories have been considered, including the one studied previously by Carlitz and Willey [7] and the one studied by Walker and Davies [22]. The other four are new and have been introduced for this study. These trajectories are all asymptotically inertial in the limit $t \to -\infty$, and all but the Carlitz-Willey trajectory are also asymptotically inertial in the limit $t \to \infty$.

For each trajectory it has been possible to obtain analytically the Bogolubov coefficients $\beta_{\omega\omega'}$ as well as the proper acceleration and the energy flux $\langle T_{uu}\rangle$. As pointed out by Walker [11], it is very useful to have models in which it is possible to do analytic calculations. The four new types of trajectories that we have provided fit this description.

Our main focus has been on the use of wave packets, which allow the particle production to be time resolved, and, in principle, might allow significant simultaneous frequency resolution as well. The packets we use form a complete orthonormal set, so that no information is lost. By computing the Bogolubov coefficients for the packets and integrating over the frequencies of the *in* modes, it is possible to obtain the average number of particles reaching $\mathcal{I}^+$ found in a given frequency range and an approximate time range (more specifically, a range in the null coordinate u). Thus, this method of analysis can be thought of as similar to what a series of particle detectors along a large υ surface would detect if each was turned on for some relatively short period of time.

In principle, one might expect a correlation between the time dependence of the particle production and the energy flux $\langle T_{uu}\rangle$. However, both vacuum polarization and particle production effects are combined in the stress-energy tensor, and it is difficult if not impossible to separate them. The use of the wave packet formalism allows for an unambiguous description of the time dependence of the particle production process.

The Carlitz-Willey trajectory was designed to result in a constant flux of energy and is of a different nature than the other trajectories in being asymptotically null. We found an explicit mathematical expression for this trajectory in terms of the Lambert W function. Because of the constant flux of energy, the total energy produced is divergent. Not surprisingly, it is also found that the number of particles produced per frequency interval $\langle N_\omega\rangle$ is also divergent.

This trajectory was the only one for which we were able to compute the number $\langle N_{jn}\rangle$ of particles associated with a wave packet analytically. Just as the energy flux is constant, we found that $\langle N_{jn}\rangle$ is independent of the value of n and so is time independent. A divergence occurs for the case $j = 0$ but not for larger values of j. This infinity can be dealt with by simply ignoring the lowest frequency ($j = 0$) bin. In a realistic detector, there will always be an infrared cutoff, since it is impossible to detect particles of arbitrarily long wavelengths. An exploration of the effects on the frequency range for the wave packets with $j > 0$ was carried out, and it was found that a Planck-type spectrum is approached in the limit that the frequency width of the packets vanishes.

The modified Carlitz-Willey trajectory has the same approximate behavior as the Carlitz-Willey trajectory at early times but then stops accelerating and approaches a constant velocity at late times. As with the Carlitz-Willey trajectory, the number of particles produced per frequency interval $\langle N_\omega \rangle$ is divergent for all ω. The energy flux $\langle T_{uu} \rangle$ is approximately constant at early times, and this results in an infinite amount of total energy E_{st}. Using wave packets we again find that $\langle N_{jn} \rangle$ is divergent for $j = 0$ but finite for all other values of j. For $j > 0$ we find that, as a function of the time parameter n, $\langle N_{jn} \rangle$ is approximately constant at early times and decreases to zero at late times as would be expected for a trajectory that is asymptotically inertial.

The Arctx and Walker-Davies trajectories are the only ones for which the mirror begins and ends at rest. We find a finite number of particles $\langle N \rangle$ is produced for both along with a finite amount of energy E_{st}. Using wave packets we have shown that the number of particles produced, $\langle N_{jn} \rangle$, increases to a maximum and then decreases over the range of time that the mirror's acceleration is first increasing and then decreasing at a significant rate.

For the Darcx and Proex trajectories, the mirror begins at rest and is asymptotically inertial in the future. In the Darcx case, it approaches a constant speed that is less than that of light, and in the Proex case, it approaches the speed of light but in such a way that it is not asymptotic to a null trajectory. For these trajectories there is an infrared divergence in the number of particles produced but not in the energy of the produced particles. However, there is no divergence in $\langle N_{jn} \rangle$ for $j = 0$. We find that the number of particles first increases to a maximum and then decreases during the period when the acceleration is first increasing and then decreasing at a significant rate.

It is interesting to compare the results for the time-dependent particle production with the average energy flux $\langle T_{uu} \rangle$. Not surprisingly, for the Carlitz-Willey trajectory, both are constant in time, so in that sense there is a correlation. For the modified Carlitz-Willey class of trajectories, there is a similar correlation at early times. Once the number of particles produced begins decreasing, the correlation diminishes and even disappears due to a flux of negative energy that occurs at intermediate times. For the other trajectories, probably again because of the fluxes of negative energy during certain time periods, there is little or no correlation between the number of particles produced and the energy flux.

Because the wave packets tile both the time and frequency domains, it might be expected that one could obtain time-dependent spectra for the particle production. For each type of trajectory (except Carlitz-Willey), the time and frequency ranges of the bins were varied. It was found (at least for these trajectories) that simultaneous time and frequency resolution with significant particle buildup in each domain is absent. The mirrors have a single-dimensional parameter that determines both the characteristic frequency and duration of creation, and for this reason the uncertainty principle prevents one from measuring the spectral dynamics. It may be possible to find mirror trajectories with two characteristic scales, one that sets the acceleration and characteristic frequency and one that sets a duration of creation. This would allow significant particle creation in the spectral dynamics to be measured by wave packets. We have not found such a trajectory. Conversely, it may be a generic feature of the quantum nature of accelerating mirrors. Our results are in two dimensions, not four. However, it seems unlikely that this effect of the uncertainty principle is tied to the number of dimensions. If our results are pointing to a generic effect, then it could have important observational consequences for any experiments that might attempt to detect the radiation produced when a mirror accelerates.

ACKNOWLEDGMENTS

M. R. R. G. appreciates helpful discussions with Xiong Chi, Paul Davies, Adam Kelleher, Laura Mersini-Houghton, and Ryan Rohm. P. R. A. acknowledges helpful discussions with Jason Bates and Sarah Fisher. M. R. R. G. acknowledges support from the U.S. Department of Education GAANN Fellowship Program Grant No. P200A090135. C. R. E. acknowledges support from the Bahnson Fund at the University of North Carolina–Chapel Hill. This work was supported in part by the National Science Foundation under Grants No. PHY-0556292 and No. PHY-0856050 to Wake Forest University.

[1] B. S. DeWitt, Phys. Rep. **19**, 295 (1975).
[2] S. A. Fulling and P. C. W. Davies, Proc. R. Soc. A **348**, 393 (1976).
[3] P. C. W. Davies and S. A. Fulling, Proc. R. Soc. A **356**, 237 (1977).
[4] P. Candelas and D. Deutsch, Proc. R. Soc. A **354**, 79 (1977).
[5] L. H. Ford and A. Vilenkin, Phys. Rev. D **25**, 2569 (1982).
[6] W. G. Unruh and R. M. Wald, Phys. Rev. D **25**, 942 (1982).
[7] R. D. Carlitz and R. S. Willey, Phys. Rev. D **36**, 2327 (1987).
[8] R. Golestanian and M. Kardar, Phys. Rev. A **58**, 1713 (1998).

[9] S. Mukohyama and W. Israel, Phys. Rev. D **62**, 121501 (2000).
[10] D. N. Page, arXiv:gr-qc/0101009.
[11] W. R. Walker, Phys. Rev. D **31**, 767 (1985).
[12] A. D. Helfer, Phys. Rev. D **63**, 025016 (2000).
[13] W. R. Walker, Classical Quantum Gravity **2**, L37 (1985).
[14] P. C. W. Davies, Phys. Lett. **113B**, 215 (1982).
[15] C. Braggio, G. Bressi, G. Carugno, C. D. Noce, G. Galeazzi, A. Lombardi, A. Palmieri, G. Ruoso, and D. Zanello, Europhys. Lett. **70**, 754 (2005).
[16] W.-J. Kim, J. H. Brownell, and R. Onofrio, Phys. Rev. Lett. **96**, 200402 (2006).
[17] C. M. Wilson, G. Johansson, A. Pourkabirian, M. Simoen, J. R. Johansson, T. Duty, F. Nori, and P. Delsing, Nature (London) **479**, 376 (2011).
[18] J.-C. Jaskula, G. B. Partridge, M. Bonneau, R. Lopes, J. Ruaudel, D. Boiron, and C. I. Westbrook, Phys. Rev. Lett. **109**, 220401 (2012).
[19] S. W. Hawking, Commun. Math. Phys. **43**, 199 (1975).
[20] M. Dorca and E. Verdaguer, in *Proceedings of the Relativity Meeting '93: Relativity in General, Salas, Spain, 1993* (unpublished).
[21] A. Fabbri and J. Navarro-Salas, *Modeling Black Hole Evaporation* (Imperial College Press, London, England, 2005).
[22] W. R. Walker and P. C. W. Davies, J. Phys. A **15**, L477 (1982).
[23] N. D. Birrell and P. C. W. Davies, *Quantum Fields in Curved Space* (Cambridge University Press, Cambridge, England, 1982).
[24] M. R. R. Good, Ph.D. thesis, University of North Carolina at Chapel Hill, 2011.
[25] F. Wilczek, arXiv:hep-th/9302096.
[26] M. Reuter and C. T. Hill, Ann. Phys. (N.Y.) **195**, 190 (1989).
[27] H. Nyquist, Phys. Rev. **32**, 110 (1928).